

Organic Functionalization of Germanium Nanowires using Arenediazonium Salts

Gillian Collins,^{†,‡} Peter Fleming,^{†,‡} Colm O'Dwyer,[§] Michael A. Morris,^{†,‡} and Justin D. Holmes^{†,‡,*}

[†]Materials and Supercritical Fluids Group, Department of Chemistry and the Tyndall National Institute, University College Cork, Cork, Ireland

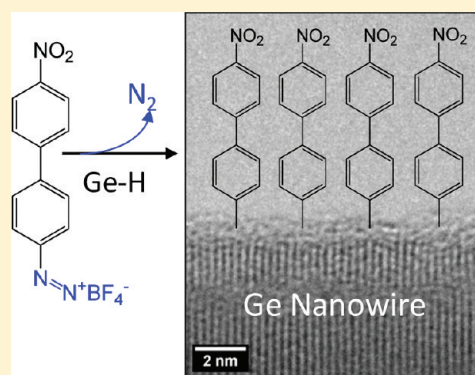
[‡]Centre for Research on Adaptive Nanostructures and Nanodevices (CRANN), Trinity College Dublin, Dublin 2, Ireland

[§]Department of Physics and Materials and Surface Science Institute (MSSI), University of Limerick, Limerick, Ireland

 Supporting Information

ABSTRACT: The formation of organic functionalization layers on germanium (Ge) nanowires was investigated using a new synthetic protocol employing arenediazonium salts. Oxide-free, H-terminated Ge nanowires were immersed in diazonium salt/acetonitrile solutions and the molecular interface of the functionalized nanowires was analyzed by reflectance infrared spectroscopy and X-ray photoelectron spectroscopy. The morphology of the modified nanowires was investigated by electron microscopy. Surface functionalization of the nanowires was found to be slow at room temperature, but proceeded efficiently with moderate heating (50 °C). The use of arenediazonium salts can result in the formation of aryl multilayers, however the thickness and uniformity of the organic layer was found to be strongly influenced by the nature of the substituents on the aromatic ring. Substituents attached to the 3-, 4-, and 5-ring positions hindered the formation of multilayers, while the presence of sterically bulky ring substituents affected the homogeneity of the organic layers. We successfully demonstrate that arenediazonium salts are very flexible precursors for nanowire functionalization, with the possibility to covalently attach a wide variety of aromatic ligands, offering the potential to alter the thickness of the resulting outer organic shell.

KEYWORDS: Nanomaterials, Semiconductors, Surface and Interfacial Phenomena



INTRODUCTION

Nanowires exhibit extremely large surface-to-volume ratios and consequently surface reactivity plays an important role in determining their chemical and electrical properties. The germanium (Ge)/GeO_x interface is characterized by a high density of surface defects and Ge displays a complex oxidation chemistry.^{1,2} Unlike Si, which possesses one stable oxide (SiO₂), Ge forms oxides in the 2+ (GeO) and 4+ (GeO₂) oxidation states. Schmeisser et al.³ carried out synchrotron studies on planar Ge surfaces and reported the presence of all four oxidation states. The composition of the surface oxide is strongly dependent on the oxidative environment, for example, dry oxidation favors the formation of Ge²⁺, while the presence of water vapor gives rise to the formation of higher Ge oxidation states.⁴ Furthermore, oxidation of the Ge surface is greatly accelerated by exposure to UV light, producing predominately GeO₄.⁵ Surface oxides are typically removed by treatment with aqueous HF, producing a hydrogen-terminated surface but the stability of the H-passivation layer under ambient conditions is limited to a few minutes before reoxidation of the surface starts to occur.^{6–8} GeO_x can also be removed by treatment with the other halogenic acids, HCl, HBr, and HI, yielding oxide free surfaces passivated by the corresponding halogen species.^{9,10}

Cullen and co-workers¹¹ first reported organic functionalization of Ge in 1962 when they demonstrated the attachment of ethyl groups via Grignard reagents to Cl-terminated Ge surfaces. Wet organic functionalization of Ge has been limited to the attachment of relatively simple ligands including alkanes,^{11–17} alkenes^{18,19} and alkanethiols.^{19–24} There are a number of drawbacks associated with many of the methodologies utilized for the surface functionalization of Ge, for example hydrogermylation reactions require relatively high reaction temperatures (>200 °C),¹⁸ alkyl Grignard reagents often require long reaction times (6 h to 8 days).²⁵ Furthermore, the reactive nature of Grignard reagents makes them incompatible with organic functionalities containing acidic protons (alcohols, carboxylic acids, amines), thereby limiting their use to relatively simple aliphatic ligands. The ability to introduce a range of chemical functionalities is essential for the integration of nanowires for electrical, chemical and biological applications. One strategy that has proved effective for the functionalization of several surfaces is the use of arenediazonium salts. Arenediazonium salts can be easily synthesized from their

Received: December 15, 2010

Revised: February 8, 2011

Published: March 04, 2011

corresponding amines, from which there are a huge range of diverse and commercially available precursors. Attachment of organic ligands by electrochemical reduction of diazonium salts is well established on carbon,^{26–28} metal,^{29,30} and oxide^{31,32} surfaces. Covalent grafting of ligands can also be initiated by chemical reduction with hypophosphorous acid³³ and metal catalysts.³⁴ There have also been reports of spontaneous attachment of aromatic ligands onto carbon,^{35–37} metal,^{38–42} and semiconductor surfaces,^{43–46} making diazonium salts a promising functionalization approach.

He et al.^{47,48} demonstrated that the electronic properties of planar Si could be altered by attaching organic molecules with different electron donating abilities. Tailoring the transport properties via surface functionalization is highly advantageous for Ge nanowires, where the use of conventional dopants, such as diborane, is known to negatively affect the nanowire morphology.⁴⁹

As far as we are aware, the reactivity of arenediazonium salts toward Ge surfaces has not been reported in the literature. Furthermore, there has been little investigation into how the presence of ring substituents influence the formation of the chemically grafted functionalization layer. In this paper we report the covalent attachment of organic ligands, via arenediazonium salts, onto H-terminated Ge nanowire surfaces. X-ray photoelectron spectroscopy (XPS) and attenuated total reflectance infrared (ATR-IR) spectroscopy were utilized to probe the organic ligands, derived from arenediazonium salts, at the nanowire surfaces. The morphology of the functionalized nanowires was investigated by scanning electron microscopy (SEM) and transmission electron microscopy (TEM). We also explore the effects of the aromatic ring substituents on the structure and uniformity of the functionalization layer.

■ EXPERIMENTAL SECTION

Ge Nanowire Synthesis. Gold-seeded Ge nanowires were synthesized on Si substrates by the thermal decomposition of diphenyl germane (purchased from ABCR) in supercritical toluene at a temperature of 400 °C and a pressure of 24.1 MPa. Details of the experimental setup are described elsewhere.⁵⁰ After synthesis, the nanowires were rinsed with chloroform, hexane, and isopropyl alcohol (IPA) and dried under Ar. The nanowires had diameters ranging from 20 to 120 nm, with a mean diameter of ~80 nm and displayed a predominate (111) growth direction with (110) and (112) growth directions also present. The nanowires examined were mostly cylindrical in nature, however a significant proportion of the (111) and (110)-oriented nanowires exhibited hexagonal cross sections displaying {110}, {111}, and {100} surface facets.^{13,51,52}

General Procedure for the Diazotization of Anilines. The arenediazonium tetrafluoroborate salts were synthesized from the corresponding anilines according to literature procedures.⁴⁴ All glassware was cleaned with aqua regia, dried overnight in an oven at 180 °C, and allowed to cool down under a N₂ atmosphere. Diethyl ether (Et₂O) was distilled from sodium/benzophenone. Acetonitrile (MeCN) was distilled from calcium hydride onto freshly prepared molecular sieves (3 Å). Anhydrous methanol (MeOH) was purchased from Sigma-Aldrich. In a glovebox, nitrosodium tetrafluoroborate (NOBF₄, purchased from ABCR) (1.1 mol equiv per aniline) was added to a Schlenk flask and sealed with a rubber septum. A minimum amount of anhydrous MeCN was added to dissolve the salt and the solution was cooled to –30 °C using a *p*-xylene-liquid N₂ cooling bath. Separately, the aniline was added to a 2-neck round-bottom flask and degassed with N₂ for 30 min. A minimum amount of MeCN was added to dissolve the aniline and the

solution was cooled to 0 °C. The organic solution was transferred to the salt solution dropwise via a cannula. After the addition, the solution was left at –30 °C for ~30 min. The temperature was raised to 0 °C and anhydrous Et₂O was added slowly until the product precipitated out of solution. The product was collected by filtration and washed with anhydrous Et₂O (× 3). The arenediazonium salts displayed good stability in air but decomposed on exposure to light. The salts were wrapped in alumina foil to prevent photochemical decomposition and stored in a freezer (–20 °C). Prior to the nanowire functionalization reactions the diazonium salts were recrystallized from cold anhydrous Et₂O.

Synthesis of 3,4,5-Trifluorophenyl Diazonium Tetrafluoroborate. 150 mg (0.6 mmol) of 3,4,5-trifluoroaniline was dissolved in 1 mL of MeCN and converted to its benzenediazonium (BD) salt following the general procedure previously described to give a very pale yellow solid in a 89% yield. IR (KBr): 2324 cm^{–1} ($\nu_{\text{N}=\text{N}}$), 1617 cm^{–1}, 1411 cm^{–1} ($\nu_{\text{C}=\text{C}}$), 1220 cm^{–1} (ν_{CF}). ¹H NMR (400 MHz, CDCl₃): δ 8.42 (d, 2H).

Synthesis of (Heptadecafluorooctyl)phenyl Diazonium Tetrafluoroborate. 200 mg (0.4 mmol) of heptadecafluorooctyl aniline was dissolved in 2 mL of MeCN and sonicated briefly. The aniline was converted into the corresponding BD salt by the procedure described to afford a colorless solid with a 76% yield. IR (KBr): 2320 cm^{–1} ($\nu_{\text{N}=\text{N}}$), 1415 cm^{–1} ($\nu_{\text{C}=\text{C}}$), 1150–1240 cm^{–1} (ν_{CF}). ¹H NMR (400 MHz, CDCl₃): δ 8.42 (dd, 2H) 7.73 (dd, 2H).

Synthesis of 4-Nitrobiphenyldiazonium Tetrafluoroborate. 100 mg (0.46 mmol) of 3,4-amino-4'-nitrobiphenyl was dissolved in ~5 mL of MeCN, sonication was required to completely dissolve the aniline, which was converted to the corresponding BD salt according to the general procedure described to give a very pale yellow colored solid with a 67% yield. IR (KBr) 2355 cm^{–1}, 2270 cm^{–1} ($\nu_{\text{N}=\text{N}}$), 1518 cm^{–1} as ($\nu_{\text{N}=\text{O}}$) 1350 cm^{–1} s ($\nu_{\text{N}=\text{O}}$), 1580 cm^{–1} ($\nu_{\text{C}=\text{C}}$), 3068 cm^{–1} ($\nu_{\text{C}-\text{H}}$). ¹H NMR (400 MHz, CDCl₃): δ 7.72 (m, *J* = 8.5, 4.7, 1.4 Hz, 2H), 7.85 (m, *J* = 8.5, 4.7, 1.4 Hz, 2H), 8.05 (dd, *J* = 8.8, 4.8 Hz, 2H), 8.51 (dd, 2H).

General Procedure for Ge Nanowire Functionalization using Arenediazonium Salts. Ge nanowires were functionalized on Si substrates from which they were grown and later removed for analysis. The native Ge oxide was first removed by immersing the nanowires into 5% aqueous HF solution for 5 min. The nanowires were then rinsed with deionized water, dried with Ar and transferred into a N₂ glovebox (<1 ppm O₂). The nanowires were immersed in freshly prepared diazonium salt solutions (1–5 mM) in anhydrous deoxygenated MeCN. Functionalization reactions were carried out at room temperature in a glovebox, or at 50 °C on a Schlenk line under a N₂ atmosphere. Reaction times ranging from 0.5, 2, 12, and 24 h were used. During the functionalization procedure the nanowires were protected from exposure to light by alumina foil to avoid the possibility of photochemical decomposition, as diazonium salts are known to be light sensitive. However, no differences in the XPS and IR spectra were observed when the reaction apparatus was not protected from light. After functionalization the nanowires were immersed in MeCN, soaked for 5 min and then rinsed with more MeCN. This soaking/rinsing procedure was repeated three times to remove unreacted or physisorbed products. The nanowires were then washed with anhydrous MeOH followed by drying under a stream of N₂.

Materials Characterization. Scanning electron microscopy (SEM) images were acquired on a FEI Inspect F, operating at 5 kV accelerating voltage. Transmission electron microscopy (TEM) images were acquired on a Jeol 2100 operating at voltage 200 kV accelerating voltage. X-ray photoelectron spectroscopy (XPS) analysis was conducted on a VSW Atom tech System with a twin anode X-ray source (Al/Mg). Survey spectra were captured at a pass energy of 100 eV, a step size of 0.7 eV and a dwell time of 0.1 ms. The core level spectra were an average of 15 scans captured at a pass energy of 50 eV, a step size of 0.2 eV and a dwell time of 0.1 ms. The spectra were corrected for charge

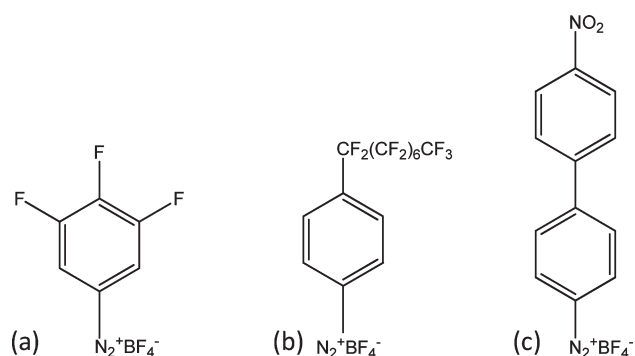


Figure 1. Structures of arenediazonium salts investigated for Ge nanowire functionalization: (a) 3,4,5-trifluorobenzenediazonium (F₃-BD), (b) heptadecafluorooctyl benzenediazonium tetrafluoroborate (F₁₇C₈-BD) and (c) nitrobiphenyldiazonium tetrafluoroborate (NO₂Ph-BD).

shift by reference to C 1s line at a binding energy of 284.8 eV. The photoemission data was processed using a Shirley background correction and peaks were fitted to Voigt profiles. The Ge 3d signals were fit to two peaks with a spin-orbit coupling of 0.585 eV and an intensity ratio of 3:2, corresponding to the Ge 3d_{5/2} and Ge 3d_{3/2} at binding energies of 28.9 and 29.5 eV (fwhm 1.5 eV), respectively. Attenuated total reflectance Fourier transfer Infrared (ATR-FTIR) analysis was carried out using a PerkinElmer spectrum 100 fitted with an ATR attachment containing a ZnSe crystal. The spectra were averaged over 10 scans at a resolution of 2 cm⁻¹. For the analysis, the nanowires were removed from the Si substrate and transferred to the ATR crystal.

Figure 1 illustrates the various diazonium salts that were investigated for surface functionalization of Ge nanowires: (a) 3,4,5-trifluorobenzenediazonium tetrafluoroborate (F₃-BD), (b) heptadecafluorooctyl benzenediazonium tetrafluoroborate (F₁₇C₈-BD) and (c) nitrobiphenyldiazonium tetrafluoroborate (NO₂Ph-BD). Fluorine substituents make excellent analytical reporting groups for XPS, having high photoionization cross sections, as well as exhibiting strong and characteristic IR absorptions. Similarly, nitro groups display strong IR vibrations and the XPS binding energy of the nitrophenyl group is easily distinguished from other N-containing functionalities. As well as ease of identification, the nature of the ring substituents of each diazonium salt differs considerably, for example F₁₇C₈-BD contains an electron withdrawing group (EWG), while F₃-BD displays electron donating mesomeric effects and electron withdrawing inductive effects. These properties are significant as EWGs are known to influence the ease of reduction of the diazonium group, and consequently may affect reactivity toward the Ge surface.⁵³ Additionally, other factors influencing nanowire functionalization such as the location of the ring substituents and steric effects of the diazonium salts are compared.

RESULTS AND DISCUSSION

Figure 2(a)(i) displays the Ge 3d core level spectrum of untreated Ge nanowires exposed to air for 12 h after synthesis. The Ge 3d_{5/2} and Ge 3d_{3/2} doublet peaks are located at binding energies of 28.9 and 29.5 eV, respectively, as well as four chemically shifted peaks located at higher binding energies which are associated with the four oxidation states of Ge.³ Figure 2(a)-(ii) and (iii) displays Ge 3d XPS data of H-terminated Ge nanowires after reaction with compounds F₁₇C₈-BD and F₃-BD at 50 °C for 6 h. The spectra of the functionalized Ge nanowires treated with the diazonium salt solutions were predominately oxide free, but trace amounts of Ge¹⁺ were present. To identify if the oxide peak was associated with the

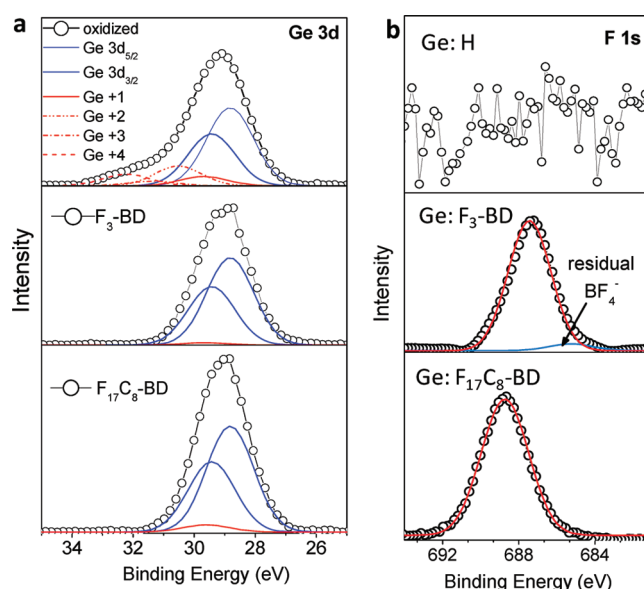


Figure 2. (a) Ge 3d XPS core level spectra of the oxidized and functionalized Ge nanowires and (b) the F 1s XPS core level spectra of H-terminated Ge nanowires and after reaction with arenediazonium salts.

functionalization procedure or originated from postfunctionalization oxidation, Ge nanowires functionalized with F₃-BD were exposed to ambient conditions for 6 h before carrying out XPS analysis. The air protected and ambient exposed samples contained similar amounts of Ge¹⁺ oxide as determined by the Ge 3d:Ge¹⁺ XPS peak intensity (see Supporting Information (SI), Figure S1), indicating that the oxide is most likely stemming from the HF treatment.⁸ Functionalization was also accompanied by the appearance of the F 1s peak in the XPS data, as shown Figure 2(b). Nanowires modified with F₃-BD showed the F 1s peak centered at a binding energy of 688 eV, typical of aromatic fluorocarbons (=C-F).⁵⁴ For nanowires treated with F₁₇C₈-BD, the F 1s peak is located at a higher binding energy of 689 eV, consistent with the presence of aliphatic fluorocarbon chains (-CF₂).⁵⁵ There was no or only trace amounts of inorganic fluorides, that is, BF₄⁻, present at a binding energy of 685 eV, suggesting that the BF₄⁻ group is no longer associated with the ligand.

The presence of organic ligands is also indicated by the C 1s XPS core level spectra, as shown in Figure 3. Fluorocarbons induce a large chemical shift in the C 1s spectra which can be seen in Figure 3 at binding energies of 288.6 eV (=C-F), 290.3 eV (-CF₂) and 292.3 eV (-CF₃).⁵⁶ The presence of an aliphatic carbon signal at 284.6 eV, most likely originates from adventitious carbon contamination and residual carbon species from the nanowire synthesis and the functionalization reactions. Similarly, the C-O signal possibly originates from solvents used in the reaction synthesis or the functionalization procedure such as IPA, or due to hydrocarbons physisorbed on top of the functionalization layer.²⁵

Figure 4 illustrates an N 1s XPS core level spectrum of Ge nanowires after reaction with NO₂Ph-BD at 50 °C. The appearance of two peaks in the N 1s spectrum is well reported in the literature for surfaces functionalized with nitrophenyl-containing compounds.^{28,34,57} The peak located at a binding energy of 405.9 eV is characteristic of the NO₂ group, whereas the second peak located at a lower binding energy of 399 eV

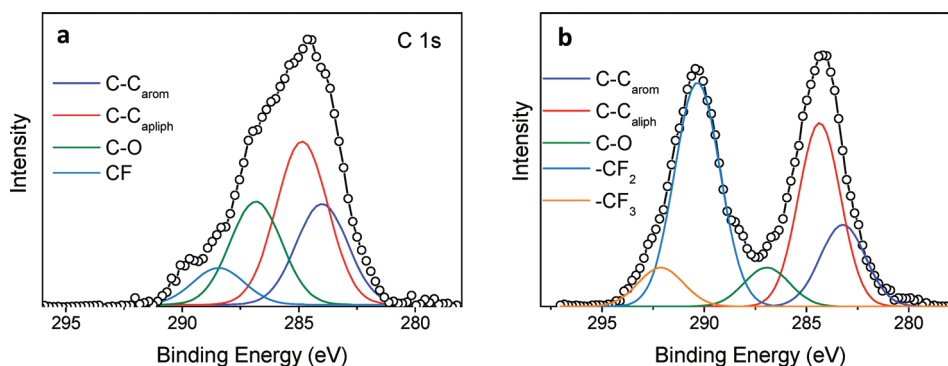


Figure 3. C 1s XPS core level spectra of Ge nanowires functionalized with (a) F₃—BD and (b) F₁₇C₈—BD.

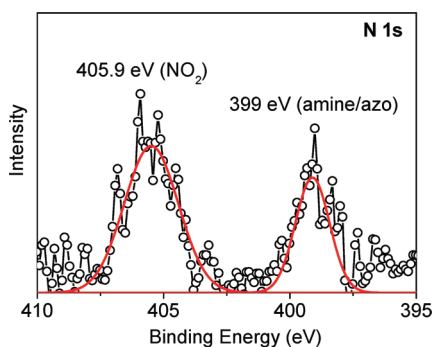


Figure 4. N 1s XPS core level spectrum of H-terminated Ge nanowires functionalized with NO₂Ph—BD.

corresponds to a reduced form of nitrogen. Several groups have attributed the latter peak to the reduction of the NO₂ group to amines (—NH₂) under the XPS beam.^{41,58} Lud and co-workers⁵⁹ found that the intensity of the peak increased with exposure to X-ray irradiation. A decrease in the NO₂ group peak intensity was observed after several XPS scans indicating that irradiation induced reduction plays a role in the presence of the peak at 399 eV. However, studies have also associated the peak at ~400 eV to the presence of azo (N = N) or azoxy (N = N—O) species, which are incorporated into the functionalization layer during the reaction.^{28,60,61} Importantly, the absence of a peak associated with the diazonium group (N≡N⁺) at ~402 eV,⁶² suggests that the salt has reacted with the Ge surface.

FTIR Analysis of Functionalized Ge Surfaces. Figure 5 compares the IR spectra of the bulk arenediazonium salts and the ATR-IR spectra after reaction with H-terminated Ge nanowires, at 50 °C. The IR spectra of H-terminated Ge nanowires, shown in Figure 5(a) consists of a broad vibrational stretch located at ~2050 cm⁻¹, which corresponds to the presence of mono-, di- and trihydride species.^{13,18} The Ge nanowire spectra display several structural features associated with the passivating ligands. Figure 5(a) illustrates the spectra of Ge nanowires treated with NO₂Ph—BD. The symmetric (ν_s) and asymmetric (ν_{as}) NO₂ stretches are observed at 1346 cm⁻¹ and 1522 cm⁻¹, respectively.⁶³ The C=C stretching vibration is also observed at 1597 cm⁻¹. Notably, there is a disappearance of the vibrational band at 2250 cm⁻¹, characteristic of the N₂⁺ group and the absence of the strong broad absorption peak for BF₄⁻, located at ~1050 cm⁻¹.⁴¹ The absence of these features is consistent with the XPS analysis and suggests the diazonium salt moiety (N₂⁺BF₄⁻) is no longer associated with the ligands.

Figure 5(b) displays the ATR-IR spectra of F₁₇C₈—BD salt and functionalized Ge nanowires. The spectral signature of the C—F bonds can be observed in the region ranging from 1100 to 1300 cm⁻¹. The CF₂ symmetric (ν_s CF₂) and asymmetric (ν_{as} CF₂) stretching vibrations occur at 1150 cm⁻¹ and 1240 cm⁻¹, respectively, as well as the bending modes (δ (CC)) at 1206 cm⁻¹.⁶⁴

Figure 6(a) compares the IR spectra for the starting aniline, the diazonium salt and functionalized Ge nanowires. Similar to spectra shown in Figure 5(a), the absence of vibrational bands attributed to the N₂⁺ and BF₄⁻ groups in the functionalized Ge nanowires suggest a reaction with the surface. The nanowire spectrum displays the presence of the =C—F absorption at 1242 cm⁻¹, typical of aromatic fluorocarbons,⁶⁵ as well as the presence of the C=C stretching vibration at 1518 cm⁻¹. Due to the high electronegativity of F substituents, the intensity of the C—H in-plane bending vibration is greatly enhanced and this can be seen in all of the spectra at 1020 cm⁻¹.⁶⁶

Reaction of the F₃—BD diazonium salt with the Ge surface can also be detected indirectly from its electronic impact on the C—H out-of-plane bending vibrations. The C—H bending vibrations are very informative about the nature of the substituents attached to the aromatic ring.⁶⁶ Figure 6(b) illustrates the C—H out-of-plane bending vibrations for the starting aniline, the diazonium salt and functionalized Ge nanowires. The aniline displays a C—H bend at 832 cm⁻¹ and after conversion into the diazonium salt the position of the vibration shifts to 866 cm⁻¹. This shift to higher frequencies is consistent with the attachment of the highly electron-withdrawing N₂⁺ group.⁶³ After reaction with H-terminated Ge nanowires, the position of the C—H bend shifts back to a lower frequency (830 cm⁻¹), as illustrated in Figure 6(b), providing indirect evidence that the diazonium functionality is no longer associated with the ligand.

SEM and TEM of Surface Modified Ge Nanowires.

Figure 7(a)–(c) display SEM images of Ge nanowires before and after treatment with arenediazonium salt solutions and shows that the functionalization procedure did not significantly affect the nanowire morphology. Figure 8(a) displays a TEM image of an untreated, oxidized Ge nanowire with a typical oxide thickness of 2–4 nm. Nanowires functionalized by immersion into NO₂Ph—BD solutions for 2 h and 12 h are compared in Figure 8(b) and (c), respectively. A reaction time of 2 h yields a thin (1.5–2 nm) homogeneous organic layer on the nanowire surface. After a 12 h reaction time, the thickness of the organic film increases to ~4 nm, accompanied by a slight decrease in uniformity relative to the thinner functionalization layer. TEM analysis suggests the presence of aryl multilayers, which form as a

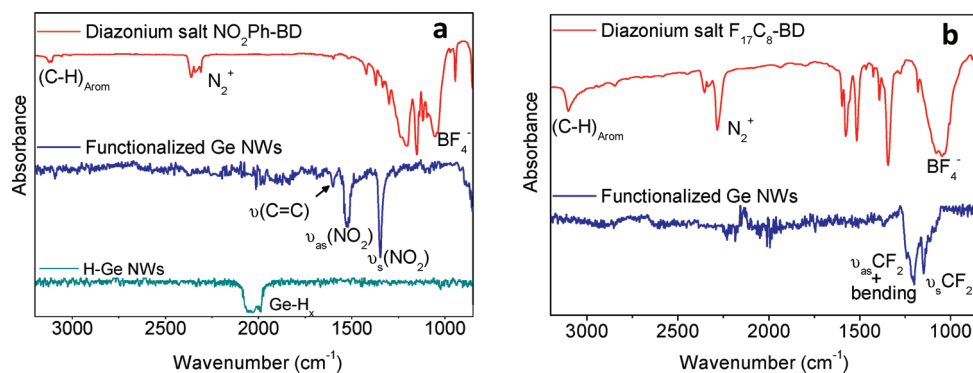


Figure 5. IR spectra of bulk diazonium salts and the ATR-IR spectra of Ge nanowires functionalized by (a) NO_2Ph —BD and H-termination, (b) F_{17}C_8 —BD.

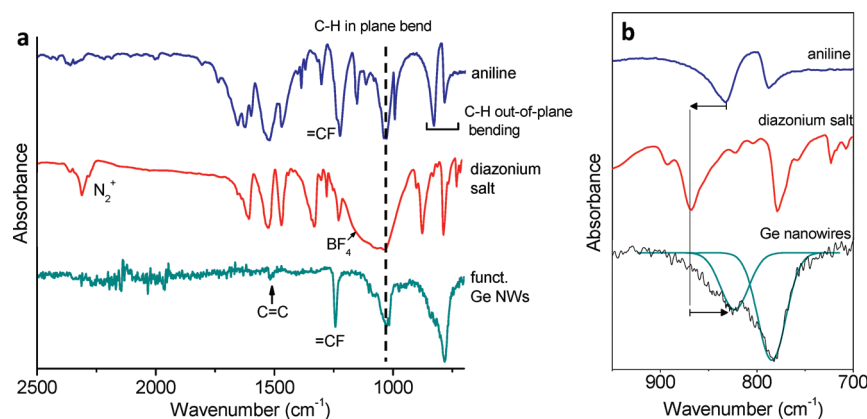


Figure 6. ATR-IR spectra of (a) trifluoroaniline, the corresponding diazonium salt (F_3 —BD) and functionalized Ge nanowires and (b) spectra illustrating the frequency shifts in the aromatic C—H out of plane bending modes.

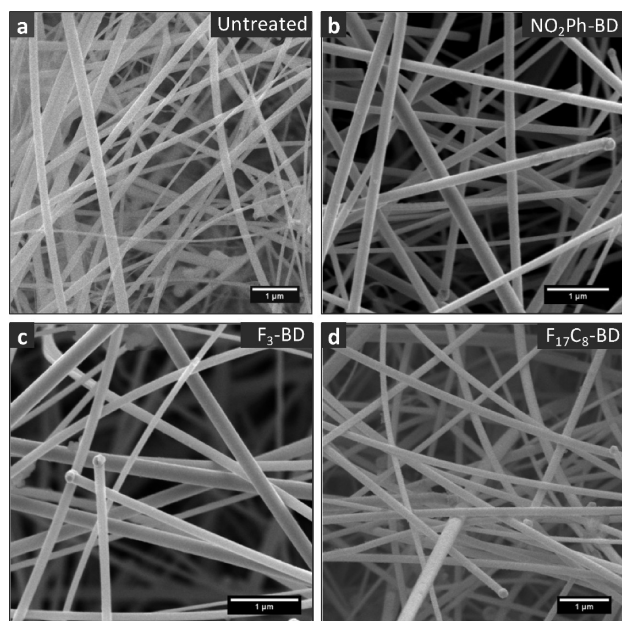


Figure 7. SEM images of (a) oxidized Ge nanowires and nanowires treated with acetonitrile solutions of (b) NO_2Ph —BD, (c) F_3 —BD, and (d) F_{17}C_8 —BD.

result of an aryl radical attaching to an already covalently bound ligand, as illustrated in Figure 8(d). Diazonium ligands grafted

electrochemically can yield organic layers ranging from nanometer to micrometer thickness^{67,68} and similarly, multilayer formation has also been reported with electroless surface modification.^{44,69}

The addition of aryl radicals to form multilayers proceeds preferentially via attack at the 3- and 5-ring positions (numbered relative to the diazonium group). A Ge nanowire modified with F_3 —BD, in which the 3-, 4-, and 5-ring positions contain F substituents, is shown in Figure 9(a). The influence of ring substituents on multilayer formation is apparent from the thickness of the functionalization layer; after a 12 h reaction time the organic layer remains thin (~ 1 nm) and does not undergo multilayer formation as observed with NO_2Ph —BD. Side reactions with F_3 —BD can only proceed via radical attack on the 2- and 6-positions, which is disfavored by steric constraints from the nanowire surface, as illustrated by the schematic shown in Figure 9(a). Podvorica and co-workers⁷⁰ reported that electrografting of aryl ligands with bulky *t*-butyl substituents on the 3- and 5-ring positions producing ultrathin organic layers close to monolayer thickness, on Si surfaces.

Figure 9(b) shows a TEM image of the functionalization layer obtained on Ge nanowires treated with F_{17}C_8 —BD for 12 h. There is a large variation in the thickness of the functionalization layer along the length of the nanowire, ranging from ~ 2 to 10 nm. The poor uniformity of the organic layer can be attributed to the sterically bulky fluorocarbon segment attached to the aromatic ring, which disrupts the packing of the aryl layers as illustrated in Figure 9(b).

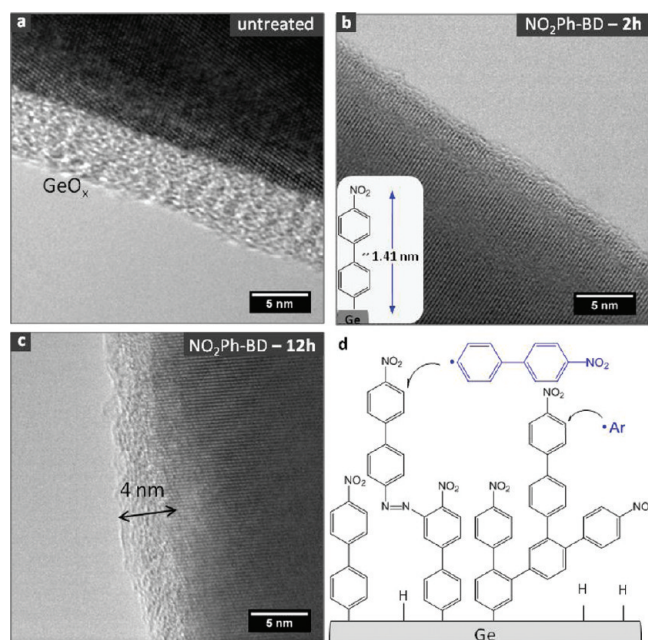


Figure 8. TEM images of (a) nonfunctionalized Ge nanowire, (b) Ge nanowire functionalized with NO₂Ph—BD after 2 h reaction time, (c) NO₂Ph—BD functionalized Ge nanowire after 12 h reaction time and (d) schematic illustrating the formation of aryl multilayers and possible introduction of azo species during multilayer formation.⁴⁵

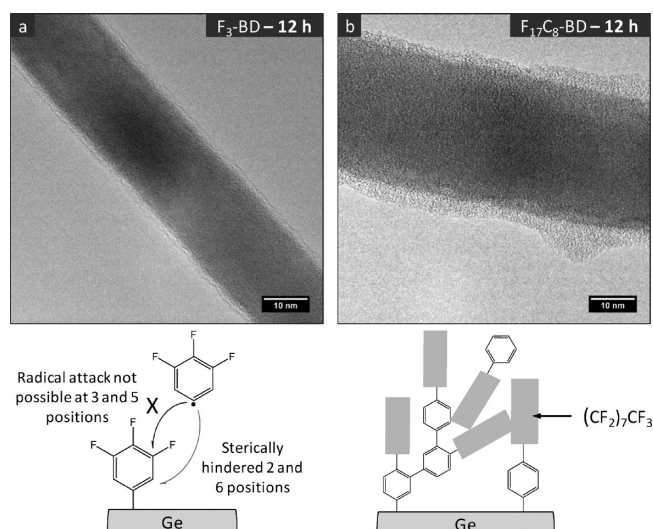


Figure 9. TEM image of Ge nanowire modified with (a) F₃—BD, (b) F₁₇C₈—BD and schematics illustrating the influence of ring substituents on the formation of organic functionalization layers.

Influence of the Reaction Time and Temperature. Functionalization reactions were carried out at 50 °C and at room temperature to investigate if a spontaneous reaction with the H—Ge surface was possible. XPS analysis found that only one of the diazonium salts investigated in the study, F₁₇C₈—BD, underwent reaction with the H—Ge surface at ambient temperature (~25 °C). The relative amount of F present at 25 and 50 °C, obtained from the integral intensity of the Ge 3d: F 1s spectra was ~2.5 times smaller at room temperature compared to the nanowires functionalized at 50 °C (see SI), indicating that the reaction is less favorable at lower temperatures. Similarly, no

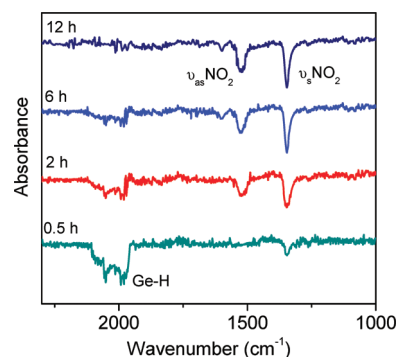


Figure 10. ATR-IR spectra of H-terminated Ge nanowires immersed in NO₂Ph—BD solutions at 50 °C for 0.5 h, 2 h, 6 and 12 h.

N 1s signal was detected for Ge nanowires treated with NO₂Ph—BD at room temperature (SI Figure S3). While both F₃—BD and NO₂Ph—BD did not display significant reaction with the Ge surface at room temperature, the reaction did proceed at 50 °C. The reduction potential of the diazonium moiety was dependent on the nature of the ring substituents; electron withdrawing substituents on the *para*-position increase the ease by which diazonium salts can be reduced.⁷¹ Studies have shown that electrochemical reduction of diazonium salts containing electron withdrawing substituents occurs faster and at less negative reduction potentials, compared to salts containing electron donating substituents.⁷² Fluorocarbons are electron withdrawing groups and the presence of a fluorocarbon chain located at the *para*-position should give rise to the easier reduction of the diazonium group and consequently result in reaction with the Ge surface at room temperature.

Haight and co-workers⁷³ observed that simply spraying a mist of diazonium salt/MeCN solution onto Si nanowires was adequate to achieve spontaneous surface functionalization, illustrating a very efficient reaction between the diazonium salt and the surfaces of the Si nanowires. The influence of the reaction time for Ge nanowire functionalization was investigated and Figure 10 displays the IR spectra of nanowires treated with NO₂Ph—BD at 50 °C for 0.5, 2, 6, and 12 h. After 2 h an absorption peak attributed to the NO₂ stretching vibrations at 1345 and 1520 cm⁻¹ was observed. There was also a Ge—H vibrational stretch present as a broad peak in the range of 1990–2050 cm⁻¹. After longer immersion times (6 and 12 h), the intensity of the Ge—H vibrational stretch decreases. Both XPS and IR data indicated that reaction of diazonium salts on Ge nanowire surfaces required elevated temperatures and longer reaction times, relative to Si surfaces. Stewart et al.⁴⁴ suggested that the presence of a highly reactive Si—H surface may play a role in activating the diazonium reaction. Si(100) surfaces treated with aqueous HF solution are known to give rise to a mainly dihydride terminated surface,⁷⁴ whereas Ge(100) surfaces tend to yield a more complex mixture of monohydride, dihydride species as well as small amounts of trihydride,⁶ which may influence the reactivity of diazonium salts toward the Ge surface. The IR spectra of H-terminated Ge nanowires consists of a broad peak centered at ~2050 cm⁻¹, which is indicative of the mono-, di-, and trihydride species.

Mechanism of Attachment. The synthetic utility of arene-diazonium salts as precursors for surface functionalization is based on the ease of reduction of the diazonium group. There are two possible reaction mechanisms by which diazonium salts can

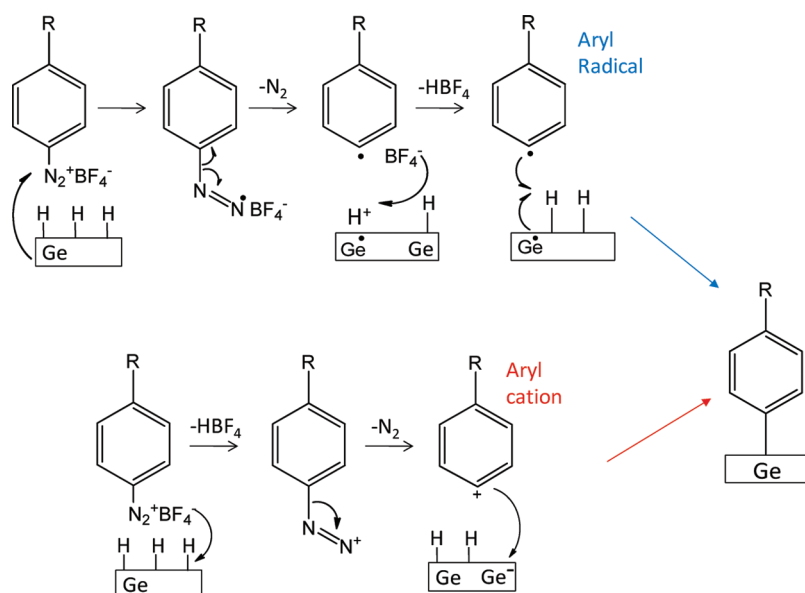


Figure 11. Reaction scheme outlining two possible reaction mechanisms for the covalent attachment of aryl ligands to H-terminated Ge nanowires based on the formation of an aryl radical or aryl cation.⁴⁸

react with the H-terminated Ge surface and are illustrated in Figure 11. The first is heterolytic dediazonation producing an aryl cation, a mechanism which involves hydrogen abstraction from the H—Ge surface.⁵³ However, germanes have a greater H-donor ability than silanes⁷⁵ and so a hydrogen-abstraction mechanism would imply that the reaction would proceed faster on a H—Ge surface than on a H—Si surface, which was not the case observed here. Furthermore, organo silyl (R_3Si-H) and stannyls (R_3Sn-H) hydrides do not react with diazonium salts via hydride abstraction and it is likely that germyl hydrides also exhibit this trend in reactivity.⁷⁶

The second possible reaction mechanism involves homolytic dediazonation. This reaction pathway involves electron transfer from the Ge surface (or possible trace impurities) to the arene-diazonium salt forming an aryl diazenyl radical, which then loses N_2 to yield an aryl radical.⁵³ Stewart and co-workers⁴⁴ provided evidence for this mechanism by observing that the introduction of a radical scavenger reduced the thickness of the functionalization layers on semiconductor surfaces. Wang and Buriak⁷⁷ conducted radical trapping experiments and showed the spontaneous electron reduction of diazonium salts in the presence of H-terminated planar and porous Si, produces surface Si radicals. A radical mechanism would be more favorable at a H-terminated Si surface than a H-terminated Ge surface due to the greater polarization of the Si—H bond,^{24,78} which may account for the lower reactivity observed at Ge surfaces. Furthermore, a homolytic dediazonation mechanism is consistent with our observation that only $F_{17}C_8-BD$, underwent spontaneous reaction with the H—Ge surface. The formation of aryl radicals is favored by the presence of electron withdrawing substituents at the *para*-position, as is the case with the fluorocarbon chain in $F_{17}C_8-BD$.⁷⁹ TEM analysis indicates the presence of thin aryl multilayers and this observation is suggestive of a radical mechanism.^{72,80}

While a radical mechanism similar to that observed for Si surfaces may be responsible for the spontaneous grafting to Ge nanowires, heating of the diazonium salts solutions was required to induce grafting of NO_2Ph-BD and F_3-BD ligands and so thermal initiation clearly plays a role in the functionalization

procedure. Thermal decomposition of arene-diazonium salts can proceed through the formation of aryl radicals or cations and many factors such as solvent polarity, ring substituents and the reaction atmosphere (N_2 versus O_2), are known to influence the mechanistic pathway and the reaction products.⁸¹ While further studies are required to fully elucidate the mechanism, a combination of thermally induced dediazonation in solution, the presence of a highly reactive Ge—H surface and possibly the presence of trace impurities from the nanowire synthesis may all contribute to the covalent grafting of aryl ligands on Ge nanowire surfaces.

CONCLUSIONS

Organic surface functionalization of Ge nanowires using diazonium salts was investigated. XPS and ATR-FTIR results indicate that functionalization of H-terminated Ge nanowire surfaces is possible through the decomposition of arene-diazonium salts in MeCN solutions. XPS and ATR analysis clearly identifies the spectral signatures of the functionalization ligands on the Ge nanowires while also indicating the loss of the N_2^+ and BF_4^- functional groups. The nature of the ring substituents was found to influence the structure of the organic functionalization layer obtained on the Ge nanowires. For monosubstituted arene-diazonium salts the thickness of the organic layer increases with reaction time due to the formation of aryl multilayers. Highly substituted aromatic rings however, resulted in thin functionalization layers as multilayer formation is hindered. Furthermore, sterically crowded ring substituents produce poorly uniform functionalization layers. The results here illustrate the potential of arene-diazonium salts as precursors for the functionalization of Ge nanowires, which may allow for the controlled growth of multilayer thin films or organic monolayers on the nanowire surface.

ASSOCIATED CONTENT

S Supporting Information. Additional information including Figures S1–S3. This material is available free of charge via the Internet at <http://pubs.acs.org>.

AUTHOR INFORMATION

Corresponding Author

*Tel: +353 (0)21 4903608; Fax: +353 (0)21 4274097; E-mail: j.holmes@ucc.ie.

ACKNOWLEDGMENT

This work was financially supported by the Irish Research Council for Science and Engineering Technology (IRCSET) and Science Foundation Ireland (Grant 08/CE/I1432). Part of this work was conducted under the framework of the INSPIRE programme, funded by the Irish Government's Programme for Research in Third Level Institutions, Cycle 4, National Development Plan 2007-201. We would also like to thank Michael Schmidt in the Electron Microscopy and Analysis Facility (EMAF) at the Tyndall National Institute, Ireland, for help with HRTEM imaging.

REFERENCES

- Zyubin, A. S.; Mebel, A. M.; Lin, S. H. *J. Chem. Phys.* **2005**, *123* (4), 044701.
- Hanrath, T.; Korgel, B. A. *J. Phys. Chem. B* **2005**, *109* (12), 5518.
- Schmeisser, D.; Schnell, R. D.; Bogen, A.; Himpsel, F. J.; Rieger, D. *Surf. Sci.* **1986**, *172*, 455.
- Prabhakaran, K.; Ogino, T. *Surf. Sci.* **1995**, *325*, 263.
- Amy, S. R.; Chabal, Y. J., Passivation and Characterisation of Germanium Surfaces. In *Advanced Gate Stacks for High-Mobility Semiconductors*; Springer: Berlin, 2007; Vol. 27.
- Rivillon, S.; Chabal, Y. J.; Amy, F.; Kahn, A. *Appl. Phys. Lett.* **2005**, *87*, 253101.
- Park, K.; Lee, Y.; Lee, J.; Lim, S. *Appl. Surf. Sci.* **2008**, *254*, 4828.
- Sun, Y.; Liu, Z. L.; Peterson, S.; Pianetta, P. *Appl. Phys. Lett.* **2006**, *88*, 021903.
- Lu, Z. H. *Appl. Phys. Lett.* **1996**, *68* (4), 520.
- Jagannathan, H.; Kim, J.; Deal, M.; Kelly, M.; Nishi, Y. *ECS Trans.* **2006**, *3* (7), 1175.
- Cullen, G. W.; Amick, J. A.; Gerlich, D. *J. Electrochem. Soc.* **1962**, *109*, 124.
- Sharp, I. D.; Schoell, S. J.; Hoeb, M.; Brandt, M. S.; Stutzmann, M. *Appl. Phys. Lett.* **2008**, *92*, 223306.
- Hanrath, T.; Korgel, B. A. *J. Am. Chem. Soc.* **2004**, *126*, 15466.
- Wang, D.; Dai, H. *Appl. Phys. A: Mater. Sci. Process.* **2006**, *85*, 217.
- Choi, H. C.; Buriak, J. M. *Chem. Commun.* **2000**, 1669.
- He, J.; Lu, Z. H.; Mitchell, S. A.; Wayner, D. D. M. *J. Am. Chem. Soc.* **1998**, *120*, 2660.
- Knapp, D.; Brunschwig, B. S.; Lewis, N. S. *J. Phys. Chem. C* **2010**, *114* (28), 12300.
- Choi, K.; Buriak, J. M. *Langmuir* **2000**, *16* (20), 7737.
- Holmberg, V. C.; Korgel, B. A. *Chem. Mater.* **2010**, *22* (12), 3698.
- Kosuri, M. R.; Cone, R.; Li, Q. M.; Han, S. M.; Bunker, B. C.; Mayer, T. M. *Langmuir* **2004**, *20* (3), 835.
- Han, S. M.; Ashurt, R.; Carraro, C.; Roy, M. *J. Am. Chem. Soc.* **2001**, *123*, 2422.
- Ardalan, P.; Musgrave, C. B.; Bent, S. F. *Langmuir* **2009**, *25*, 2013.
- Wang, D.; Chang, Y.-L.; Liu, Z.; Dai, H. *J. Am. Chem. Soc.* **2005**, *127*, 11871.
- Ardalan, P.; Sun, Y.; Pianetta, P.; Musgrave, C. B.; Bent, S. F. *Langmuir* **2010**, *26* (11), 8419.
- Bashouti, M. Y.; Stelzner, T.; Christiansen, S.; Haick, H. *J. Phys. Chem. C* **2009**, *113*, 14823.
- Allongue, P.; Delamar, M.; Desbat, B.; Fagebaume, O.; Hitmi, R.; Pinson, J.; Saveant, J. M. *J. Am. Chem. Soc.* **1997**, *119* (1), 201.
- Kuo, T. C.; McCreery, R. L.; Swain, G. M. *Electrochem. Solid St. Phys.* **1999**, *2* (6), 288.
- Yu, S. S. C.; Tan, E. S. Q.; Jane, R. T.; Downard, A. J. *Langmuir* **2007**, *23* (22), 11074.
- Stockhausen, V.; Ghilane, J.; Martin, P.; Trippé-Allard, G.; Randriamahazaka, H.; Lacroix, J. C. *J. Am. Chem. Soc.* **2009**, *131* (41), 14920.
- Boukema, K.; Chehimi, M. M.; Pinson, J.; Blomfield, C. *Langmuir* **2003**, *19* (15), 6333.
- Maldonado, S.; Smith, T. J.; Williams, R. D.; Morin, S.; Barton, E.; Stevenson, K. J. *Langmuir* **2006**, *22* (6), 2884.
- Merson, A.; Dittrich, T.; Zidon, Y.; Rappich, J.; Shapira, Y. *Appl. Phys. Lett.* **2004**, *85* (6), 1075.
- Toupin, M.; Belanger, D. *Langmuir* **2008**, *24* (5), 1910.
- Mevellec, V.; Roussel, S.; Tessier, L.; Chancolon, J.; Mayne-L'Hermite, M.; Deniau, G.; Viel, P.; Palacin, S. *Chem. Mater.* **2007**, *19* (25), 6323.
- Seinberg, J. M.; Kullapere, M.; Maeorg, U.; Maschion, F. C.; Maia, G.; Schiffrin, D. J.; Tammeveski, K. *J. Electroanal. Chem.* **2008**, *624* (1–2), 151.
- Sinitskii, A.; Dimiev, A.; Corley, D. A.; Fursina, A. A.; Kosynkin, D. V.; Tour, J. M. *ACS Nano* **2010**, *4* (4), 1949.
- Zhu, Y.; Higginbotham, A. L.; Tour, J. M. *Chem. Mater.* **2009**, *21* (21), 5284.
- Gehan, H.; Fillaud, L.; Felidj, N.; Aubard, J.; Lang, P.; Chehimi, M. M.; Mangeney, C. *Langmuir* **2010**, *26* (6), 3975.
- Chamoulaud, G.; Belanger, D. *J. Phys. Chem. C* **2007**, *111* (20), 7501.
- Combella, C.; Delamar, M.; Kanoufi, F.; Pinson, J.; Podvorica, F. I. *Chem. Mater.* **2005**, *17* (15), 3968.
- Adenier, A.; Cabot-Deliry, E.; Chausse, A.; Griveau, S.; Mercier, F.; Pinson, J.; Vautrin-UI, C. *Chem. Mater.* **2005**, *17* (3), 491.
- Adenier, A.; Barre, N.; Cabot-Deliry, E.; Chausse, A.; Griveau, S.; Mercier, F.; Pinson, J.; Vautrin-UI, C. *Surf. Sci.* **2006**, *600* (21), 4801.
- Pinson, J.; Podvorica, F. *Chem. Soc. Rev.* **2005**, *34*, 429.
- Stewart, M. P.; Maya, F.; Kosynkin, D. V.; Dirk, S. M.; Stapleton, J. J.; McGuinness, C. L.; Allara, D. L.; Tour, J. M. *J. Am. Chem. Soc.* **2004**, *126* (1), 370.
- Charlier, J.; Golus, E.; Bureau, C.; Palacin, S. *J. Electroanal. Chem.* **2009**, *625* (1), 97.
- Haight, R.; Sekaric, L.; Afzali, A.; News, D. *Nano Lett.* **2009**, *9* (9), 3165.
- He, T.; Ding, H. J.; Peor, N.; Lu, M.; Corley, D. A.; Chen, B.; Ofir, Y.; Gao, Y. L.; Yitzchaik, S.; Tour, J. M. *J. Am. Chem. Soc.* **2008**, *130* (5), 1699.
- He, T.; He, J. L.; Lu, M.; Chen, B.; Pang, H.; Reus, W. F.; Nolte, W. M.; Nakanishi, D. P.; Franzon, P. D.; Tour, J. M. *J. Am. Chem. Soc.* **2006**, *128* (45), 14537.
- Tutuc, E.; Guha, S.; Chu, J. O. *Appl. Phys. Lett.* **2006**, *88*, 043113.
- Chlistunoff, J.; Ziegler, K. J.; Lasdon, L.; Johnston, K. P. *J. Phys. Chem. A* **1999**, *103*, 1678.
- Hanrath, T.; Korgel, B. A. *Small* **2005**, *1* (7), 717.
- Li, C.-P.; Lee, C. S.; Ma, X.-L.; Wang, N.; Zhang, R.-Q.; Lee, S.-T. *Adv. Mater.* **2003**, *15* (7), 607.
- Zollinger, H. *Angew. Chem., Int. Ed.* **1978**, *17*, 141.
- Pola, J.; Urbanova, M.; Bastl, Z.; Plzak, Z.; Subrt, J.; Gregora, I.; Vorlicek, V. *J. Mater. Chem.* **1998**, *8* (1), 187.
- Ferraria, A. M.; da Silva, J. D. L.; do Rego, A. M. B. *Polymer* **2003**, *44* (23), 7241.
- Lei, Y. G.; Ng, K. M.; Weng, L. T.; Chan, C. M.; Li, L. *Surf. Interface Anal.* **2003**, *35* (10), 852.
- Chakraborty, A. K.; Coleman, K. S.; Dhanak, V. *Nanotechnology* **2009**, *20*, 155704.
- Mendes, P.; Belloni, M.; Ashworth, M.; Hardy, C.; Nikitin, K.; Fitzmaurice, D.; Critchley, K.; Evans, S.; Preece, J. *ChemPhysChem* **2003**, *4* (8), 884.
- Lud, S. Q.; Steenackers, M.; Jordan, R.; Bruno, P.; Gruen, D. M.; Feulner, P.; Garrido, J. A.; Stutzmann, M. *J. Am. Chem. Soc.* **2006**, *128*, 16884.

- (60) Shewchuk, D. M.; McDermott, M. T. *Langmuir* **2009**, *25* (8), 4556.
- (61) Doppelt, P.; Hallais, G.; Pinson, J.; Podvorica, F.; Verneyre, S. *Chem. Mater.* **2007**, *19* (18), 4570.
- (62) Szunerits, S.; Boukherroub, R. *J. Solid State Electrochem.* **2008**, *12*, 1205.
- (63) Smith, B., *Infrared Spectral Interpretation: A Systematic Approach*; CRC Press: Boca Raton, FL, 1999;
- (64) Tsao, M. W.; Hoffmann, C. L.; Rabolt, J. F.; Johnson, H. E.; Castner, D. G.; Erdelen, C.; Ringsdorf, H. *Langmuir* **1997**, *13* (16), 4317.
- (65) Wall, L. A.; Donadio, R. E.; Pummer, W. J. *J. Am. Chem. Soc.* **1960**, *82* (18), 4846.
- (66) Coates, J., Interpretation of infrared spectra, a practical approach. In *Encyclopedia of Analytical Chemistry*; Meyers, R. A., Ed.; John Wiley & Sons Ltd.: Chichester, 2000; pp 10815.
- (67) Adenier, A.; Combellas, C.; Kanoufi, F.; Pinson, J.; Podvorica, F. I. *Chem. Mater.* **2006**, *18* (8), 2021.
- (68) Hunger, R.; Jaegermann, W.; Merson, A.; Shapira, Y.; Pettenkofer, C.; Rappich, J. *J. Phys. Chem. B* **2006**, *110* (31), 15432.
- (69) Combellas, C.; Kanoufi, F.; Pinson, J.; Podvorica, F. I. *Langmuir* **2005**, *21* (1), 280.
- (70) Combellas, C.; Kanoufi, F.; Pinson, J.; Podvorica, F. I. *J. Am. Chem. Soc.* **2008**, *130* (27), 8576.
- (71) Galli, C. *Chem. Rev.* **1988**, *88* (5), 765.
- (72) Bernard, M. C.; Chausse, A.; Cabet-Deliry, E.; Chehimi, M. M.; Pinson, J.; Podvorica, F.; Vautrin-UI, C. *Chem. Mater.* **2003**, *15* (18), 3450.
- (73) Haight, R.; Sekaric, L.; Afzali, A.; Newns, D. *Nano Lett.* **2009**, *9* (9), 3165.
- (74) Miyata, N.; Watanabe, S.; Okamura, S. *Appl. Surf. Sci.* **1997**, *117*, 26.
- (75) Chatgililoglu, C.; Ballestri, M.; Escudie, J.; Pailhous, I. *Organometallics* **1999**, *18* (12), 2395.
- (76) Nakayama, J.; Yoshida, M.; Simamura, O. *Tetrahedron* **1970**, *26*, 4609.
- (77) Wang, D.; Buriak, J. M. *Langmuir* **2006**, *22*, 6214.
- (78) Fujimoto, H.; Inagaki, S. *J. Am. Chem. Soc.* **1977**, *99* (23), 7426.
- (79) Zollinger, H., *Diazo Chemistry I: Aromatic and Heteroaromatic Compounds*; VCH: Weinheim, 1994;
- (80) Anariba, F.; Viswanathan, U.; Bocian, D. F.; McCreery, R. L. *Anal. Chem.* **2006**, *78* (9), 3104.
- (81) Canning, P. S. J.; McCrudden, K.; Maskill, H.; Sexton, B. *J. Chem. Soc., Perkin Trans. 2* **1999**, No. 12, 2735.